Experimental Heat Transfer Investigation of Tube Row Effects at Air-Side Heat Exchanger with Serrated Finned-Tubes

RENE HOFMANN, FRIEDRICH FRASZ, KARL PONWEISER
Institute of Thermodynamics and Energy Conversion
Vienna University of Technology
A-1060 Vienna, Getreidemarkt 9/E302
AUSTRIA

Abstract: Tube row effects on heat transfer at transverse serrated finned-tubes in cross-flow were investigated. The heat exchanger consists of finned-tubes, which are arranged as 8, 6, 4, 2 consecutive columns in flow direction, or as a single tube row, each consisting of 11 horizontal tubes. The tubes are arranged in a staggered formation at equal transverse and longitudinal pitch. The experimental setup, the measurement technique, and the measurement uncertainties are presented. After measurement validation, the derived correlations for the Nusselt number were compared with experimental results and equations from literature. A decreasing relative deviation with an increasing number of consecutive tube rows between counter-flow and counter cross-flow, in the formula for the calculation of the logarithmic mean temperature difference, can be seen. A reduction coefficient for finned-tube heat exchangers with few consecutive tube rows in gas flow was developed.

Key-Words: Finned-tube, Serrated fin, Heat transfer, Pressure drop, Experimental setup, Helical finned-tube, Number of consecutive tube rows, Data validation

1 Introduction

Finned-tube bundles in heat exchangers for heat recovery steam generators are very often applied with only a few consecutive tube rows in cross-flow. As tests have shown, the heat transfer coefficient at heat exchangers in staggered tube arrangement varies with the number of consecutive tube rows. The heat transfer coefficient increases at staggered arrangements with the number of consecutive tube rows in cross-flow until an almost constant value is achieved. According to different authors, this varies from 4 to 10 tube rows. Investigations presented in [17], [18], [20], [21], and [24] have shown, that for common tube arrangements in heat recovery steam generators, this critical value is reached with about 8 tube rows. The usually applied equations for heat transfer of finned-tube bundles indicate a critical value of more than 8 tube rows. For a smaller number of tube rows, a reduction coefficient arises, which is dependent on the Reynolds number. This can be applied both for tube rows with solid and serrated fins. The pressure drop coefficient on the other hand shows no distinctive dependence on the number of consecutive tube rows in cross-flow.

Experimental investigations at solid and serrated finned-tubes have been studied extensively by [1], [9], [10], [11], [12], [13], and [24]. The influence of the arrangement of finned-tubes was investigated by [2], [11], and [16]. Weierman and Taborek [16] found that in-line arrangement should only be used for special cases because of the disadvantage of possible bypass flows between the tube bundles. Bell and Kegler [2] analyzed the effect of bypassing in heat exchangers for a specific thermal performance. Briggs and Young [15] investigated several finned-tube configurations. The given heat transfer correlation is based on tubes varying widely with respect to fin height, fin thickness, fin spacing and root diameters. These equations can be used for predicting six-row deep tube banks with solid fins. Ward and Young [4] developed heat transfer and pressure drop correlations for plain finned-tubes with triangular pitches.

Numerous correlations for the prediction of heat transfer of serrated fin tubes have been derived in literature, whereas Nir´s [19] correlations are based on a large amount of heat-transfer and pressure-drop data. In [14] and [24], an excellent overview of circular finned-tube studies is presented.

In the present study a function for a reduction coefficient for finned-tube heat exchangers, depending on the number of tube rows, was developed.

2 Experimental Procedure

In Fig. 1 the layout of the test facility for heat transfer and pressure drop measurements at finned-tube bundles in cross-flow is shown. This test

facility allows measuring at Reynolds numbers in the range between 4500 and 35000.

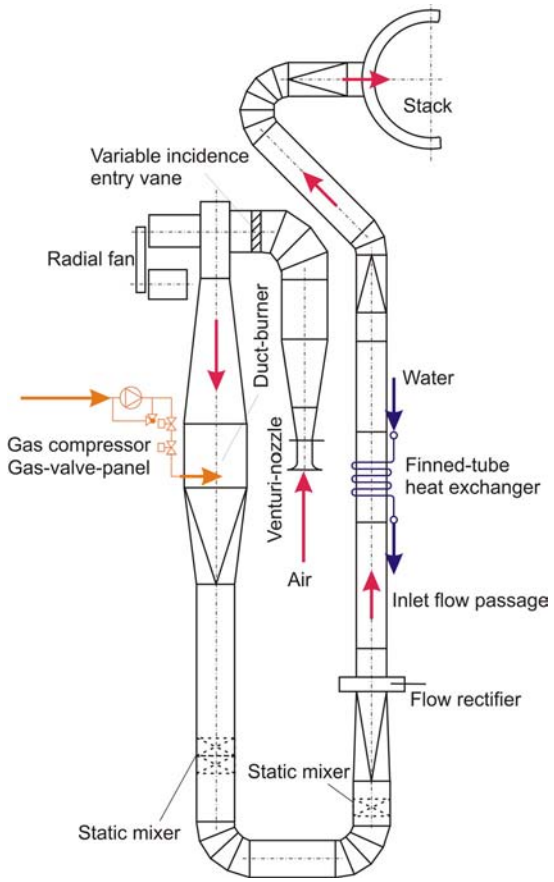

Fig.1: Sketch of the test facility

The finned-tube bundle is admitted with hot gas up to 400°C, which is generated by combustion of natural gas. Air is sucked in using a Venturi nozzle and a smaller ISA 1932 inlet nozzle for low *Re*-numbers, which are also used for mass flow measurement of combustion air. Both measurement systems were pre-calibrated before application. A variable incidence entry vane is mounted in front of the radial fan for mass flow regulation of the air. The radial fan generates 45000 Nm³/h at 3500 Pa. The burner is designed as a duct burner with a maximum power of 1160 kW. As flow regulating systems, two static mixers, a flow rectifier, which consists of three fine wire meshes in close arrangement, and a 2000 mm inlet channel, which serves to calm the fully developed turbulent flow, are installed.

The finned-tube counter cross-flow heat exchanger consists of a rectangular sheet steel channel, in which the staggered finned-tubes are arranged horizontally with a tube length of approx. 500 mm and a given transversal and longitudinal pitch. All connecting pipes are arranged at the outside of the channel. This is the only arrangement which allows exact measurement of heat transfer at the small test section width of the tube banks. Therefore, the measurements are not influenced by any bypass flow through the space for the bends. Bundles, consisting of 88, 66, 44, and 22 tubes, which were arranged in 8, 6, 4, and 2 consecutive columns in flow direction, each consisting of 11 horizontal tubes, were investigated.

In all cases for an even cooling water flow distribution in the tubes, orifices after the inlet collector are installed, for more details refer to [3]. Measurements for a single tube row were only possible due to modification of the test rig, because the system is only designed for an even number of tube rows. The characteristic parameters of the analyzed finned-tube are presented in table 1.

Fin Geometry	**U-serrated**
Bare tube diameter	38.0 mm
Tube thickness	3.2 mm
Number of fins per m	295
Average fin height	20.0 mm
Average fin thickness	0.8 mm
Average tube length	495 mm
Average segment width	4.3 mm
Number of tubes in flow-direction	8, 6, 4, 2, 1
Number of tubes per row	11
Longitudinal tube pitch	79 mm
Transversal tube pitch	85 mm
Outside surface area for 8 tube rows	84.48 m²,
for 6 tube rows	63.36 m²,
for 4 tube rows	42.24 m²,
for 2 tube rows	21.12 m²,
for 1 tube row	10.56 m²
Fin material	DC01
Tube material	St 35.8
Net free area of tube row	0.2292 m²

Table 1: Specifications of finned-tubes

Semi-tubes should be arranged on the channel wall, especially in staggered tube arrangements, in order to prevent a detrimental bypass flow through the otherwise empty space. In order to fully achieve this effect, these semi-tubes should also participate in heat transfer, which requires a very complicated design of the water side [3]. The simpler construction design, as shown in Fig. 2, is usually chosen therefore. To measure heat transfer at a lower number of parallel tube rows, i.e. 6, 4, 2 rows, or a single tube row, the tubes were removed from the downstream of the flue gas duct. In Fig. 2, a schematic sketch of four consecutive tube rows in

staggered arrangement is presented. The transversal and the longitudinal pitch are different. Thus, these measurement results differ from those cited in literature [4], with an equilateral triangular pitch.

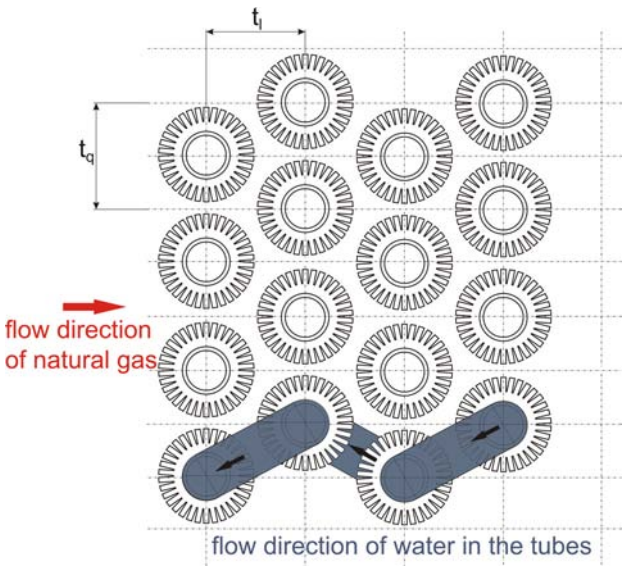

Fig.2: Staggered finned-tube arrangement

The main advantages of the U-fin geometry (Fig. 3) are a larger contact area between fin and tube (heat conduction) and a smaller fin spacing possibility, which allows a higher total outside surface area at equal fin height of the bundle. Thus, equal or smaller installation size of the heat exchanger can be achieved. The geometric dimensions of the finned-tube are presented in the schematic sectional drawing (Fig. 3).

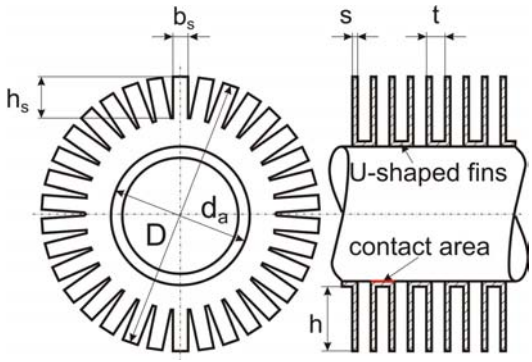

Fig.3: Investigated finned-tube with U-fins

Therein the fin pitch t is n_R^{-1}, b_s is the average segment width, h_s the average segment height, s the average fin thickness, h the average fin height, and $D = d_a + 2h$, with d_a as the bare tube diameter.

The experimental investigation requires a number of measurements to be taken simultaneously in order to evaluate and determine the amount of transferred heat as well as the gas-side pressure drop. The temperatures on the water side are measured for every coiled tube at the inlet and at the outlet using Pt-100 RTDs (resistance temperature detectors) so that fringe effects can be ascertained for the tubes near the channel wall and considered in the evaluation. Gas temperatures are measured using NiCr-Ni thermocouples. To affect the flow pattern not to significantly, the diameter of these thermocouples was chosen to be only 1.5 mm. Four thermocouples are arranged and mounted upstream as well as downstream of the heating surface of the heat exchanger to obtain a grid measurement. Three NiCr-Ni thermocouples measure the air temperature at the Venturi nozzle and after the fan as well as the gas temperature after the burner. The water mass flow is measured using a calibrated hot water meter with an electronic sensor.

Air mass flow is measured by determining the pressure difference at the Venturi nozzle in front of the inlet collector using two different sensors: a Honeywell micro-switch series 160 (±0.25% Full scale (FS)) and a Furness Controls micro-manometer. Air humidity is measured by means of an electronic humidity sensor. The barometric pressure is measured using a Honeywell HPB digital precision barometer with an accuracy of ±0.4 hPa FS. The static pressure differences at the air side of the finned-tube bundle are measured at four inlets in front of and after the heating surface of the heat exchanger, using a Honeywell PPT digital precision pressure transducer with an accuracy of ±0.05% FS.

The total pressure difference at the centre of the combustion channel is measured using a United Sensor pitot-static pressure probe. The absolute pressure in the combustion channel is measured using a Honeywell micro-switch series 160 (±0.25% FS). All measurement systems were pre-calibrated before application. The measured values are transmitted to the process computer using a data acquisition system of National Instruments and the LabView 7E program system.

3 Data Reduction

To investigate the characteristics of heat transfer of finned-tubes, the outside heat transfer coefficient must be determined. This can be done by use of energy balances. The heat flow due to the change of enthalpy of the water in the heat exchanger is

$$\dot{Q}_w = \dot{m}_w c_{p_w} (T_{w_1} - T_{w_2}) . \qquad (1)$$

The heat flow due to the change of enthalpy of the gas in the heat exchanger is

$$\dot{Q}_g = \dot{m}_g c_{p_g} (T_{g_1} - T_{g_2}). \quad (2)$$

The energy balance of water and gas must be equal.

$$\dot{Q}_g = \dot{Q}_w \quad (3)$$

The heat transfer coefficient at the inner side of the tube can be calculated with the knowledge of all data at the water-side. The volume flow of water is constant ($\dot{V}_W$=14.1 m³/h at p_W=2.7 bar) with a known uncertainty. Heat conduction through the tube wall is known as

$$\dot{Q} = kA_{tot} LMTD_C, \quad (4)$$

whereby k is the heat transfer coefficient, A_{tot} the total outside surface area of the bundle and $LMTD_C$ the logarithmic mean temperature difference between inlet and outlet of the heat exchanger. According to [8], the LMTD for a counter cross-flow heat exchanger is calculated with

$$LMTD_{CC} = \sqrt[z]{LMTD_X} \left(LMTD_C\right)^{\left(1-\frac{1}{z}\right)}. \quad (5)$$

Therein, z is the number of consecutively arranged equal crossings. Equation (5) distinguishes between cross-flow and counter-flow heat exchangers. In case of z=1, equation (5) changes into the formula for cross-flow heat exchangers

$$LMTD_X = \Theta\left(T_{g_1} - T_{w_1}\right). \quad (6)$$

The correction factor Θ is defined by the balance or imbalance of the heat exchanger [8]. If z→∞, the LMTD of a counter-flow heat exchanger is defined by

$$LMTD_C = \frac{(T_{g_1} - T_{w_2}) - (T_{g_2} - T_{w_1})}{\ln \frac{T_{g_1} - T_{w_2}}{T_{g_2} - T_{w_1}}}. \quad (7)$$

In the actual study, the LMTD is calculated using equation (7) for counter-flow heat exchangers. Figure 4 presents the relative deviation of the temperature measurement, comparing equation (5) and (7) at different tube row numbers. As shown in Fig. 4, the difference between counter-flow and counter cross-flow in the formula for the calculation of the logarithmic mean temperature difference is decreasing with an increasing number of consecutive tube rows. The figure shows also that the influence of a low number of tube rows is small. Therefore, equation (7) can be used for analyzing the measured data.

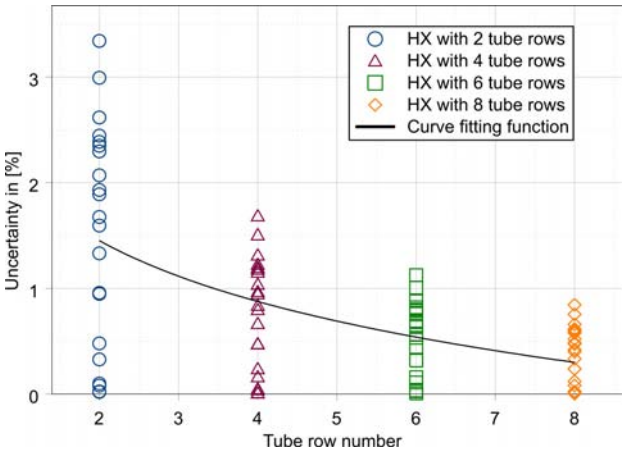

Fig.4: Relative deviation between counter cross-flow and counter-flow heat exchanger

With the knowledge of the logarithmic mean temperature difference and fluid properties, the heat transfer coefficient at the gas side can be calculated. A reduction coefficient, termed "fin efficiency" is introduced [3], by which the actual heat transfer coefficient is multiplied to obtain the apparent heat transfer coefficient. Fin efficiency is calculated according to the laws of heat conduction under the assumption that the actual heat transfer coefficient is uniformly distributed across the fin surface [3]. The apparent heat transfer coefficient is

$$\alpha = \frac{1}{\frac{1}{k} - f_a \frac{d_a}{d_i \alpha_i} - f_a \frac{d_a}{2\lambda_r} \ln \frac{d_a}{d_i}}. \quad (8)$$

With the help of fin efficiency, the current (external) heat transfer coefficient at the surface is

$$\alpha_0 = \frac{\alpha A_{tot}}{A_{tube} + \eta_r A_{fin}}. \quad (9)$$

The dimensionless Nusselt number Nu_0 with the characteristic dimension d_a at the medium gas temperature is calculated using the equation

$$Nu_0 = \frac{\alpha_0 d_a}{\lambda_b}. \quad (10)$$

For more details see [5]. The experimental uncertainty of the gas-side heat transfer coefficient was estimated by the law of error propagation of Gauss.

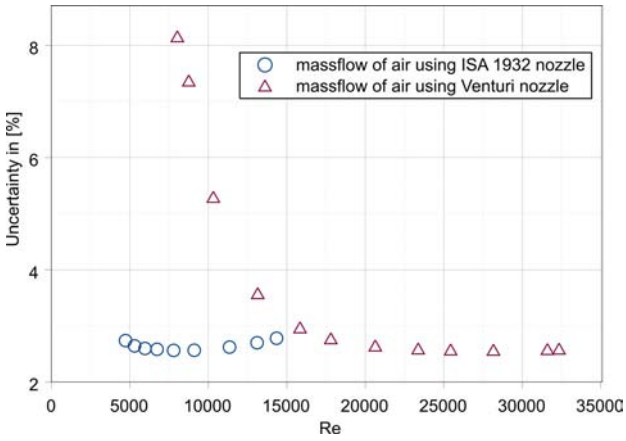

Fig.5: Mass flow measurement uncertainties

The average error of the mass flow measurement of air is about ±3-5 %. As presented in Fig. 5, a disproportionate rising at low Re-numbers (Re < 14000) occurs. In the range of 8000 < Re < 10000 the uncertainty is approximately ±10 %, and for Re < 5000 about ±15 %. For this reason an ISA 1932 inlet nozzle was applied for low mass flows.

As mentioned above, the measurements were performed at the gas-side and at the water-side. To obtain exact heat transfer correlations, each calculated point is validated after measuring, according to a validation model, introduced by J. Tenner el al. [6]. This curve fitting method uses equations of mass-balances, of energy-balances, and measurement value equations. The basic concept of the validation is to use all measured values with their variances and co-variances to fulfil all side conditions. For the chosen variables, $\dot{m}_w$, $\dot{m}_g$, T_{w1}, T_{w2}, T_{g1}, T_{g2} in equations (1) and (2), the conditions of the energy balance (3) must be met. The real measured values with their uncertainties

$$M = (M_1, M_2, M_3, \ldots) \tag{11}$$

do not satisfy the side conditions. For this reason, measured data are supplemented with correction factors. Thus we obtain the following:

$$V = M + \upsilon\,. \tag{12}$$

The corrections υ are determined in such a way that equation (13) reaches a minimum and the side condition (14) is equal to zero.

$$G(\upsilon) = \upsilon^T \sum M^{-1}\upsilon \rightarrow \text{Min} \tag{13}$$

$$h(V) = 0 \tag{14}$$

Equation (13) is the fitting function with the inverse matrix for the co-variance. All measured values are independent and the matrix of the co-variance is according to [6], [7]. After combining equation (13) and (14), and using the Lagrange multiplicator

$$\gamma = (\gamma_1, \gamma_2, \ldots\ldots, \gamma_6), \tag{15}$$

the fitting function is written as follows:

$$G(V,\gamma) = \frac{(V_1 - M_1)^2}{\sigma^2_{M_1}} + \ldots\ldots\ldots + \frac{(V_6 - M_6)^2}{\sigma^2_{M_6}} + \\ + 2\gamma\left(V_1 c_{p_w}(V_2 - V_3) - V_4 c_{p_g}(V_5 - V_6)\right) \rightarrow \text{Min}\,. \tag{16}$$

The solution of equation (16) is known as calculus of variations with side functions, according to Gauss. A system of equations for seven variables is obtained. After applying this criterion, all measured values can be developed into correlations for the prediction of the Nusselt numbers.

3 Results and Discussion

According to the method of dynamic similarity an objective function of Nusselt is defined as follows:

$$Nu = f(Re, Pr)\,. \tag{17}$$

Following dimensional analysis, the power law for the heat transfer correlation was developed.

$$Nu = C\,Re^m\,Pr^n \tag{18}$$

C and m are functions of geometric parameters, whereas n depends on the fluid properties. All Nu correlations are calculated at constant Pr values. In case of air as heat transfer medium, the thermal boundary layer is thicker than the boundary layer of fluid. The variation of Pr under test conditions is small and can therefore be neglected in further calculations.

Figure 6 shows the dimensionless heat transfer coefficient for a representative number of measured points in the Re-range of 8, 6, 4, and 2 serrated finned-tube rows in staggered arrangement and for a single tube row.

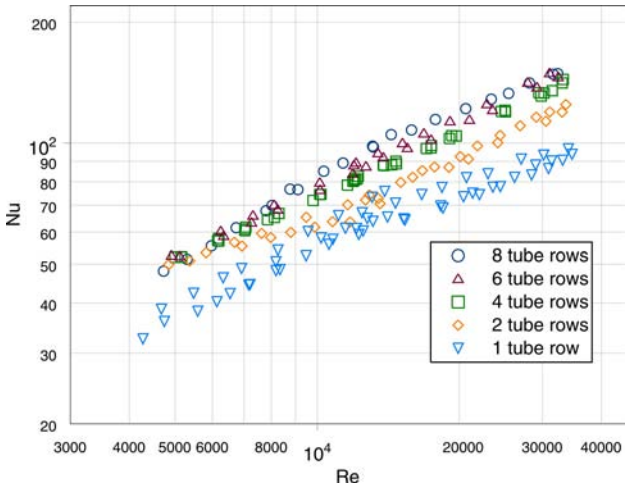

Fig.6: Heat transfer of different consecutive tube row numbers, for Pr=0.71 and d=38 mm

As seen, the heat transfer coefficient increases with an increasing number of tube rows. The Nu-number tends to be constant above 8 tube rows, see Fig. 13 and Fig. 6. The measurement uncertainty for a single tube row is high, due to low fluid temperature difference between inlet and outlet at the water-side.

Figures 7 to 10 show a comparison of the measured results at 8, 6, 4, and 2 consecutive tube rows with Weierman's correlations [17] and [9]. Additional results for 4 and 2 tube rows, compared with correlations developed by Nir [19] and VDI WA [23], are presented in Fig. 9 and 10. The VDI equations are valid only for solid finned-tubes. Thus the Nu-numbers calculated with those equations are lower than the calculated values of the investigated U-shaped finned-tubes.

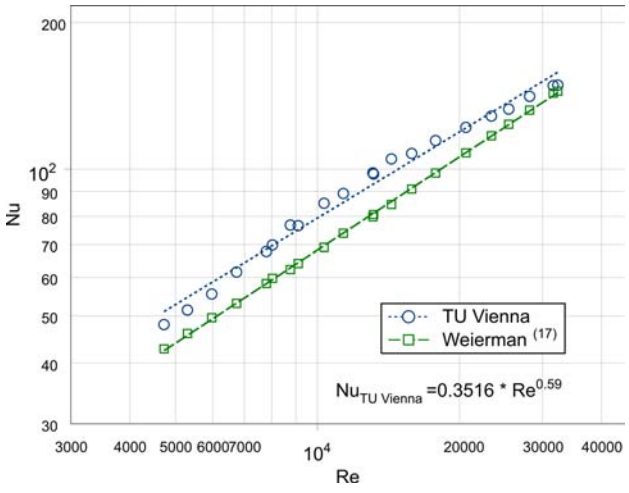

Fig.7: Comparison of heat transfer at 8 consecutive tube rows with literature, for Pr=0.71 and d=38 mm

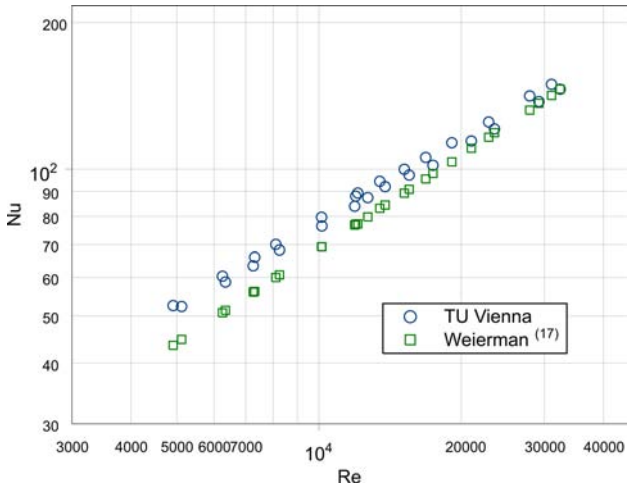

Fig.8: Comparison of heat transfer at 6 consecutive tube rows with literature, for Pr=0.71 and d=38 mm

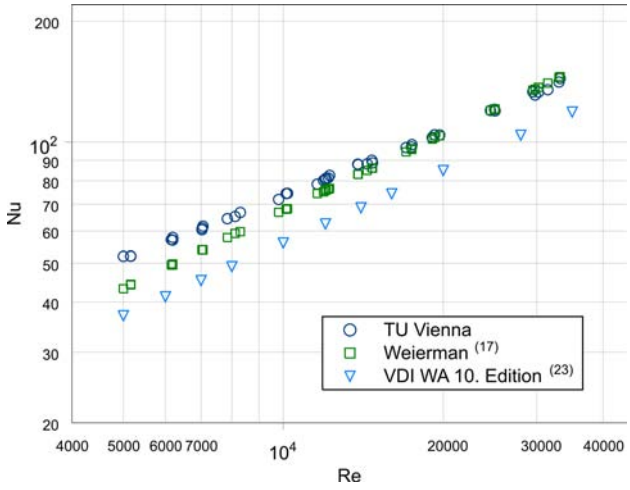

Fig.9: Comparison of heat transfer at 4 consecutive tube rows with literature, for Pr=0.71 and d=38 mm

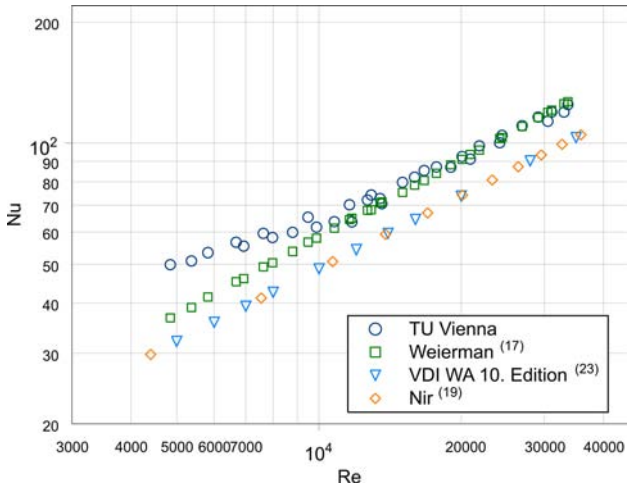

Fig.10: Comparison of heat transfer at 2 consecutive tube rows with literature, for Pr=0.71 and d=38 mm

Both the VDI correlations and characteristics of Nir show approximately the same gradient. The equations of Weierman [17] have a measurement uncertainty of about ±10 % for serrated fin tubes in a staggered equilateral layout. Thus, our results agree well with the literature. The exponents for the Nusselt correlations vary from about 0.5 to 0.6, as seen in Fig. 9 and 10. This variation could be caused by the pressure difference measurement uncertainty of the mass flow of air at low Re numbers and the temperature measurement uncertainty between inlet and outlet of the water-side and/or gas-side. The equations mentioned above are valid in general for several consecutive tube rows in cross-flow. Since two or even only one tube row occur sometimes in heat recovery boilers, heat transfer equations for one tube row are required. Figure 11 shows a comparison with literature of the heat transfer at one tube row. The heat transfer calculation at only one finned-tube row, according to VDI WA [22], is based on the calculation at a tube surrounded by the flow. The flooding length at the smooth tube is used in this case as the characteristic length. The measured results show high uncertainty. But in the measured Re-range, approximately the same gradient of the exponent in the power law (18) can be observed within the three equations.

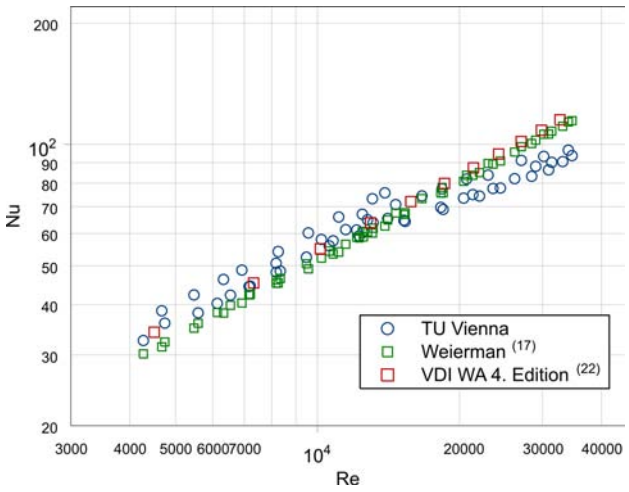

Fig.11: Comparison of heat transfer at one tube row with literature, for Pr=0.71 and d=38 mm

The formulas for heat transfer at finned-tubes are generally valid for a certain minimum number of consecutive tube rows. This number varies according to the authors from 4 to 12 tube rows at staggered tube arrangement [3]. A reduction of heat transfer at staggered tube arrangement is generally assumed for smaller number of tube rows. This reduction of the heat transfer coefficient for a small tube row number in relation to the value α_∞ (heat transfer coefficient for more than 8 tube rows) at different constant Re-Numbers is shown; Fig. 12. For the calculation of the reduction coefficient, the same method is used as seen in [3]. Yet, there is no agreement between individual authors on the tube row number at which the heat transfer coefficient remains constant.

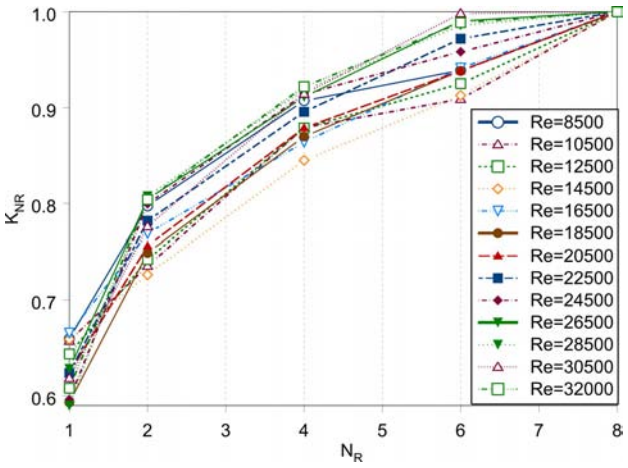

Fig.12: Reduction coefficient K_{NR} for 8, 6, 4, 2, and 1 tube rows at different Re-numbers

Depending on the longitudinal pitch t_l, the heat transfer coefficient differs for various tube bundles. Thus, different values are obtained for a heat exchanger with only one tube row by using the reduction coefficients [3]. According to Weierman [17], the reduction coefficient is stated in dependence of t_l/t_q. In Fig. 13, the mean average reduction coefficient K_{NR} is compared with [17] and [18]. As seen, there is a good congruence between our measurements and literature.

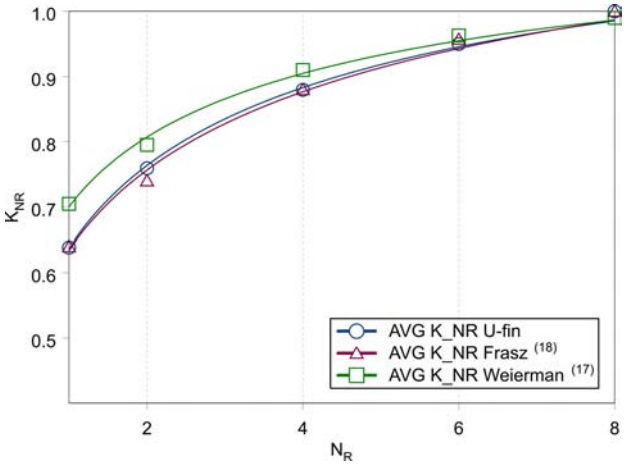

Fig.13: Mean average reduction coefficient K_{NR} for 8, 6, 4, 2, and 1 tube rows in staggered arrangement

Finned-tube heat exchangers with few consecutive tube rows in a gas flow require a correction of the heat transfer coefficient. According to [3], the Nusselt number for N_R consecutive tube rows, with N_R less than 8, is calculated as

$$Nu_{0,N_R} = Nu_{0,\infty} K_{NR} . \quad (19)$$

4 Conclusion

Heat transfer behaviour for different numbers of consecutively arranged tubes at serrated finned-tube bundles in cross-flow was investigated. All finned-tubes are arranged in a staggered way at equal transverse and longitudinal pitch. The test rig, the measurement technique, the measurement uncertainties, and the calculation with the law of error propagation of Gauss were presented.

A small difference of the logarithmic mean temperature difference compared with formulas for counter-flow and counter cross-flow was detected. In the actual study, the LMTD was calculated using the equation for counter-flow heat exchangers.

Following an analysis and an evaluation of the measured values, heat transfer correlations were determined. The derived correlations for the Nusselt number at different configurations were compared with equations from literature. This comparison revealed good congruence for high number of consecutive tube rows.

Measurements of the heat transfer at only one finned-tube row shows high uncertainty. But in the measured Re-range, approximately the same gradient of the exponent in the power law can be observed.

For a smaller number of tube rows a reduction coefficient was developed, which depends on the Reynolds number. A comparison of the obtained reduction coefficient displayed good agreement with the formulas in the literature.

Further studies, especially comparisons between measurement results at global performance and numerical investigations of local heat transfer behaviour in a single tube row (e.g. turbulences, horseshoe vortices occuring in the fluid flow between the serrated fin tips), will provide further knowledge of fluid flow and local heat transfer distribution and will give a more complete understanding of performance behaviour.

5 Nomenclature

A_{fin}	Fin surface area of the bundle	[m²]
A_{tube}	Bare tube surface area of the finned-tube bundle	[m²]
A_{tot}	Total outside surface area of the finned-tube bundle	[m²]
b_s	Segment width	[m]
c_p	Specific heat capacity	[J/kgK]
d_a	Bare tube diameter	[m]
D	Total outside diameter	[m]
f_a	Geometry factor	[-]
G(υ)	Fitting function	-
h(V)	Side function	-
h	Average fin height	[m]
h_s	Average segment height	[m]
k	Heat transfer coefficient	[W/m²K]
K_{NR}	Mean average reduction coefficient	[-]
LMTD	Logarithmic mean temperature difference	[K]
$\dot{m}$	Mass flow	[kg/s]
$M_{1..6}$	Measured values	-
N_R	Number of tubes in flow-direction	[-]
n_R	Number of fins per meter	[m^{-1}]
p	Pressure	[N/m²]
$\dot{Q}$	Heat flow	[W]
s	Average fin thickness	[m]
t	Fin pitch	[m]
t_l	Longitudinal tube pitch	[m]
t_q	Transversal tube pitch	[m]
T	Temperature	[K]
$V_{1..6}$	Corrected measurement value	-
$\dot{V}$	Volume-flow	[m³/h]
z	Number of consecutive arranged equal crossings	[-]
Nu	Nusselt number	[-]
Pr	Prandtl number	[-]
Re	Reynolds number	[-]

Greek Symbols

α	Heat transfer coefficient	[W/m²K]
$\gamma_{1..6}$	Lagrange multiplicator	-
η	Fin efficiency	[-]
λ	Thermal conductivity	[W/mK]
υ	Correction	-
$\sigma_{M1..6}$	Co-variances	[-]
Θ	Correction factor	[-]

Indices

0	Characteristic length at d_a
1	Inlet
2	Outlet
a	Outside
b	Calculation condition
c	Counter flow
cc	Counter cross-flow

g Gas
i Inside
C, m, n Function on geometric parameters and tube bundle arrangement, fluid flow
r Fin
w Water
x Cross-flow

References:

[1] T.J. Rabas, P.W. Eckels, Heat transfer and pressure drop performance of segmented extended surface tube bundles, *AIChE-ASME Heat Transfer Conference, San Francisco, California, Aug.11-13, 1975, pp. 1-8*.

[2] K.J. Bell, W.H. Kelger, Analysis of bypass flow effects in tube banks and heat exchangers, *The American Institute of Chem. Engineers*, Vol.74, No.174, 1978, pp. 47-52.

[3] F. Frasz, Principles of finned-tube heat exchanger design for enhanced heat transfer, *Heat and Mass Transfer*, WSEAS-Press, 2008.

[4] D.J. Ward, E.H. Young, Heat transfer and pressure drop of air in forced convection across triangular pitch banks of finned tubes, *Chem. Eng. Prog. Symp. Ser*, Vol.55, No.29, 1959, pp. 37-44.

[5] R. Hofmann, F. Frasz, K. Ponweiser, Experimental Analysis of Enhanced Heat Transfer and Pressure-Drop of Serrated Finned-Tube Bundles with different Fin Geometries, *in: "Theoretical and Experimental Aspects of Heat and Mass Transfer"*, WSEAS Press, pp. 54-62, 2008.

[6] J. Tenner, P. Klaus, E. Schulze, Erfahrungen bei der Erstellung und dem Einsatz eines Datenvalidierungsmodells zur Prozessueberwachung und –optimierung im Kernkraftwerk Isar 2, *VGB Kraftwerkstechnik*, Vol. 4, 1998, pp. 43-49.

[7] S. Streit, Messunsicherheit und Vertraeglichkeitspruefungen: Beispiele und vergleich mit herkoemmlichen Verfahren, *VDI-Bericht 1210*, 1995.

[8] W. Wagner, Waermeaustauscher, *Vogel-Fachbuch*, 1993.

[9] G. Breber, Heat transfer and pressure drop of stud finned tubes, *The American Institute of Chem. Engineers*, Vol.87, No.283, 1991, pp. 383-390.

[10] H. Walczyk et al., An experimental study of convective heat transfer from extruded type helical finned tubes, *Chemical Engineering and Processing*, Vol.42, 2003, pp. 29-38.

[11] F. Frasz, Waermeuebertragung in Rippenrohr-waermeaustauschern, *Waermeaustauscher, Energie-einsparung durch Optimierung von Waerme-prozessen*, Vulkan-Verlag Essen 2, 1994, pp. 70-76.

[12] R.L. Webb et al., Data reduction for air-side performance of tin-and-tube heat exchnagers, *Experimental Thermal and Fluid Science*, Vol. 21, 2000, pp. 218-226.

[13] K. Kawaguchi, Heat transfer and pressure drop characteristics of finned tube banks in forced convection, *Journal of Enhanced Heat Transfer*, Vol.12, No.1, 2005, pp. 1-20.

[14] R.L. Webb, Air-side heat transfer in finned tube heat exchangers, *Heat Transfer Engineering*, Vol. 1, Nr. 3, 1980, pp. 33-49.

[15] D.E. Briggs, E.H. Young, Convection heat transfer and pressure drop of air flowing across triangular pitch banks of finned tubes, *Chem. Eng. Prog. Symp. Ser*, Vol.59, No.41, 1963, pp. 1-10.

[16] C. Weierman, J. Taborek, W.J. Marner, Comarison of the performance of in-line and staggered banks of tubes with segmented fins, *The American Institute of Chem. Engineers*, Vol.74, No.174, 1978, pp. 39-46

[17] C. Weierman, Correlations ease the selection of finned tubes, *The Oil and Gas Journal*, Vol.74, No.36, 1976, pp. 94-100.

[18] F. Frasz, W. Linzer, Waermeuebergangs-probleme an querangestroemten Rippenrohr-buendeln, *BWK*, Vol.44, No.7/8, 1992, pp. 333-336.

[19] A. Nir, Heat transfer and friction factor correlations for cross flow over staggered finned tube banks, *Heat Transfer Eng.*, Vol.12, No.1, 1991, pp. 43-58.

[20] S. Wongwises, Y. Chokeman, Effect of fin pitch and number of tube rows on the air side performance of herringbone wavy fin and tube heat exchnagers, *Energy Conversion and Management*, Vol.46, 2005, pp. 2216-2231.

[21] J. Unk, Verfahren zur Optimierung von Rippenrohren und der Rohrreihenzahl in der Waermerueckgewinnung, *Klima-Kaelte-Heizung*, Vol.2, 1981, pp. 383-386.

[22] VDI−Waermeatlas, *4th Edition*, VDI Verlag Duesseldorf 1984.

[23] VDI−Waermeatlas, *10th Edition*, Springer Verlag, Berlin Heidelberg New York 2006.

[24] J. Stasiulevicius, A. Skrinska, Heat transfer of finned tube bundles in crossflow, *Hemisphere Publ. Corp.*, Washington New York London, 1988.